Intensity and polarization dependences of the supercontinuum generation in birefringent and highly nonlinear microstructured fibers

Antoine Proulx, Jean-Michel Ménard, Nicolas Hô, Jacques M. Laniel and Réal Vallée

COPL, Département de Physique, Université Laval, Québec, Canada, G1K 7P4
antoine.proulx@phy.ulaval.ca

Claude Paré

INO, 2740 Rue Einstein, Québec, Canada, G1P 4S4

Abstract: We present experimental results highlighting the physical mechanism responsible for the initial spectral broadening of femtosecond Ti:Sapphire pulses in a highly birefringent microstructured fiber having a small effective area. By rotating the input polarization and varying the injected power while monitoring the resulting changes in the output spectrum, we are bringing clear evidences that the initial broadening mechanism leading to a broadband supercontinuum is indeed the fission of higher-order solitons into redshifted fundamental solitons along with blueshifted nonsolitonic radiation.

References and links

1. J.K. Ranka, R.S. Windeler and A.J. Stentz, "Visible continuum generation in air-silica microstructure optical fiber with anomalous dispersion at 800 nm," Opt. Lett. **25**, 25-27 (2000).
2. A.V. Husakou and J. Hermann, "Supercontinuum generation of higher-order solitons by fission in photonic crystal fibers," Phys. Rev. Lett. **87**, 203901 (2001).
3. S. Coen, A. H. L. Chau, R. Leonhardt, J. D. Harvey, J. C. Knight, W. J. Wadsworth and P. St. J. Russell, "Supercontinuum generation by stimulated Raman scattering and parametric four-wave mixing in photonic crystal fibers," J. Opt. Soc. Am. B **19**, 753-764 (2002).
4. J. Herrmann, U. Griebner, N. Zhavoronkov, A. Husakou, D. Nickel, J.C. Knight, W.J. Wadsworth, P.St.J. Russell and G. Korn, "Experimental evidence for supercontinuum generation by fission of higher-order solitons in photonic fibers," Phys. Rev. Lett. **88**, 173901 (2002).
5. A. L. Gaeta, "Nonlinear propagation and continuum generation in microstructured optical fibers," Opt. Lett. **27**, 924-926 (2002).
6. B. R. Washburn, S. E. Ralph and R. S. Windeler, "Ultrashort pulse propagation in air-silica microstructure fiber," Opt. Express **10**, 575-580 (2002),
   http://www.opticsexpress.org/abstract.cfm?URI=OPEX-10-13-575.
7. A. V. Husakou and J. Herrmann, "Supercontinuum generation, four-wave mixing, and fission of higher-order solitons in photonic-crystal fibers," J. Opt. Soc. Am. B **19**, 2171-2182 (2002).
8. A. Ortigosa-Blanch, J.C. Knight and P. St. J. Russell, "Pulse breaking and supercontinuum generation with 200-fs pump pulses in photonic crystal fibers," J. Opt. Soc. Am. B **19**, 2567-2572 (2002).
9. G. Genty, M. Lehtonen , H. Ludvigsen, J. Broeng and K. Kaivola, "Spectral broadening of femtosecond pulses into continuum radiation in microstructured fibers," Opt. Express **10**, 1083-1098 (2002),
   http://www.opticsexpress.org/abstract.cfm?URI=OPEX-10-20-1083 .
10. K.M. Hilligsøe, H. N. Paulsen, J. Thøgersen, S.R. Keiding and J. J. Larsen, "Initial steps of supercontinuum generation in photonic crystal fibers," J. Opt. Soc. Am. B **20**, 1887-1893 (2003).
11. G.P. Agrawal, *Nonlinear Fiber Optics 3rd Ed.* (Academic Press, New York, 2001).
12. N. Akhmediev and M. Karlsson, "Cherenkov radiation emitted by solitons in optical fibers," Phys. Rev. A. **51**, 2602-2607 (1995).

13. M. Lehtonen, G. Genty, H. Ludvigsen and M. Kaivola, "Supercontinuum generation in a highly birefringent microstructure fiber," Appl. Phys. Lett. **82**, 2197-2199 (2003).
14. J.C. Knight, T.A. Birks, P.St.J. Russell and D.M. Atkin, "All-silica single-mode optical fiber with photonic crystal cladding," Opt. Lett. **21**, 1547-1549 (1996).

1. Introduction

Over the past few years, microstructured (MS) optical fibers have generated a lot of interest because of their unique and often revolutionary physical properties. One of these remarkable properties is the possibility to fabricate MS highly nonlinear fibers having a very small mode area and a zero-GVD wavelength in the operation range of some modern high peak-power pulsed lasers. The combination of these two properties resulted in a dramatic increase in the efficiency of many nonlinear processes such as self-phase modulation, four-wave mixing (FWM), Raman scattering and soliton propagation. The interplay between these nonlinear processes has been reported by several authors as being the mechanism leading to supercontinuum generation extending from the UV to the IR [1-9]. Furthermore, it has been proposed [4, 7, 9, 10] that by using laser pulses having a duration of a few hundred femtoseconds in the anomalous dispersion regime, the basic mechanism underlying the generation of broadband supercontinuum in MS fibers is the fission of higher-order solitons due to third-order dispersion, Raman scattering and self-steepening. Accordingly, the femtosecond pulse launched in the fiber initially forms a higher-order soliton, for which the order N is the closest integer given by [11]:

$$N = \sqrt{\frac{L_D}{L_{NL}}} = \sqrt{\frac{\gamma P_o}{|\beta_2|}} \frac{T_{FWHM}}{1.665} \, , \tag{1}$$

where L_D and L_{NL} are respectively the dispersion length and the nonlinear length, γ is the nonlinear coefficient of the fiber, P_o is the input peak power, T_{FWHM} is the input pulse duration and β_2 is the dispersion coefficient of the fiber at the input wavelength ($\beta_2 < 0$). Because of higher-order dispersion and nonlinear effects, this N^{th} order soliton rapidly decays into N redshifted fundamental solitons along with blueshifted non-solitonic radiation (NSR) [9]. These blue components of the spectrum find their origin in the soliton fission mechanism itself as they contain the energy radiated away from the pulses in order for them to be able to propagate as fundamental solitons [12]. This mechanism can explain very well the initial broadening of the spectrum but a more complex dynamics involving nonlinear effects such as FWM and Raman scattering along with the dispersion properties of the fiber is accountable for the generation of a broad and flat supercontinuum.

An investigation of the supercontinuum generation process in a highly birefringent MS fiber has recently been reported by Lehtonen *et al.* [13]. They observed that when the input polarization is oriented along one of the polarization axes of the birefringent fiber, the generated spectral components have the same polarization as the input light and this polarization is maintained in the course of propagation in the MS fiber. They also noticed that one can take advantage of the different dispersion characteristics of the two eigenpolarization modes to get one more degree of freedom for tailoring the generated supercontinuum. In the present paper, we present some experimental results in a format that is well suited for clearly confirming the theory according to which the fission of higher-order solitons is the fundamental mechanism underlying the initial spectral broadening. Contour plots and multimedia files of the evolution of the generated spectrum as the injected power is increased, allow us to show the complete picture of the initial spectral broadening due to the soliton self-frequency shift followed by the spectrum flattening and this, in a visually clear fashion. Also, contour plots of the changes in the spectrum resulting from a rotation of the input polarization for different injected intensities, provides an unambiguous proof that the generated spectrum at the fiber output consists of a superposition of the spectra generated independently by the two eigenpolarization modes. Such a global picture of the continuous evolution of the supercontinuum as the input power is increased and the input polarization is rotated has not

been presented before and is bringing a new dimension to our understanding of this phenomenon.

2. Experimental results and discussion

We fabricate our highly nonlinear holey fiber as part of a research project at INO. The fabrication of the fiber is done in a two-step procedure following a method previously reported in the literature [14]. The first operation consists of stacking capillaries into a hexagonal structure in which the central capillary has been replaced by a solid silica rod of same outer diameter. This structure is then placed in a silica tube and drawn into a cane of a few millimeters in diameter by using a conventional fiber optic drawing tower. This holey cane is subsequently introduced into in a tightly fitting silica tube that will form the final preform to be drawn. In order to be able to draw a 125 μm fiber having the desired core diameter, hole spacing and hole size, we have to carefully select 1) the dimensions of the capillaries used to build the initial preform, 2) the diameter of the intermediate holey cane and 3) the dimensions of the silica tube into which the cane is placed before the final preform is drawn to a fiber. The fiber used for this work consisted of two hexagonal layers of air holes surrounding a pure-silica elliptical core with dimensions of 1.3 μm x 2.3 μm, yielding an effective area $A_{eff} \sim 3$ μm^2. A scanning electron micrograph (SEM) image of this fiber is shown in Fig. 1. The modal birefringence has been measured to be 2.2×10^{-3} at a wavelength of 1530 nm.
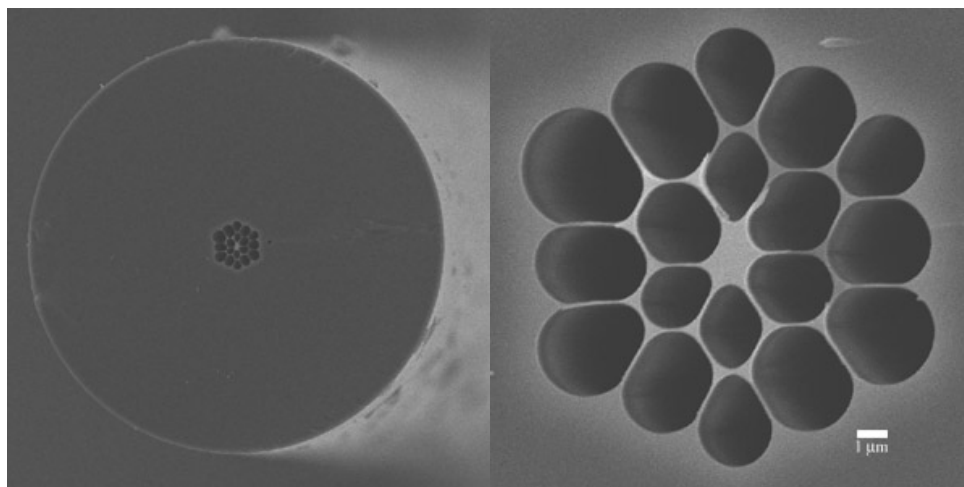

Fig. 1. SEM images of the 2 m long MS fiber used for the experiment (left) and a detailed view of its central region (right). The outer diameter of the fiber is 125 μm and the elliptical core has dimensions 1.3μm x 2.2 μm.

For the supercontinuum generation experiment, we used a commercially available mode-locked femtosecond Ti:Sapphire laser system (Spectra-Physics Tsunami) capable of developing laser pulses in the 100 femtosecond (FWHM) range at a 81 MHz repetition rate for a maximum average output power of 1W. In order to avoid any retro-reflections toward the laser, a Faraday isolator is placed just after the output of the Ti:Sapphire oscillator. While allowing an increase of the injected power in the fiber by providing more stability to the laser during the experiment, the presence of this Faraday isolator caused a slight stretching of the laser pulses. The polarization control at the fiber input was achieved by positioning a half-wave plate in front of a 40X microscope objective used to inject the laser pulses in the 2 m long holey fiber. The coupling efficiency has been measured to be to be around 25-30%. The supercontinuum generated in the MS fiber was recorded using an optical spectrum analyzer

(Ando AQ6115E). The experiments were performed at wavelengths of 740 nm and 758 nm. These wavelengths are located near the zero dispersion wavelengths (ZDW) on the anomalous dispersion side for each of the eigenpolarization modes of the fiber.

The supercontinua were generated by injecting 192 fs laser pulses (FWHM) at a wavelength of 758 nm and an intensity of 56 GW/cm^2 (peak power/effective area) along the two eigenpolarization axes of the fiber. The resulting spectra for both polarization axes are shown in Fig. 2. When injecting the laser with a polarization parallel to the fast and slow axes of the fiber, we could infer, from the position of the dips in the spectra [9], ZDW values of 625 nm and 645 nm respectively. In Fig. 2, it is worth noting that by injecting the laser pulses polarized parallel to the slow axis of the fiber, we are able to generate a very broad and flat supercontinuum. From 765 to 1365 nm, the generated spectrum is flat within a 3 dB range. Also note that the abrupt cut of the spectrum in the longer wavelengths is attributable to the OH absorption peak at 1380 nm, it should be possible to achieve even wider supercontinua with such a flatness by reducing the OH absorption of the MS fiber.
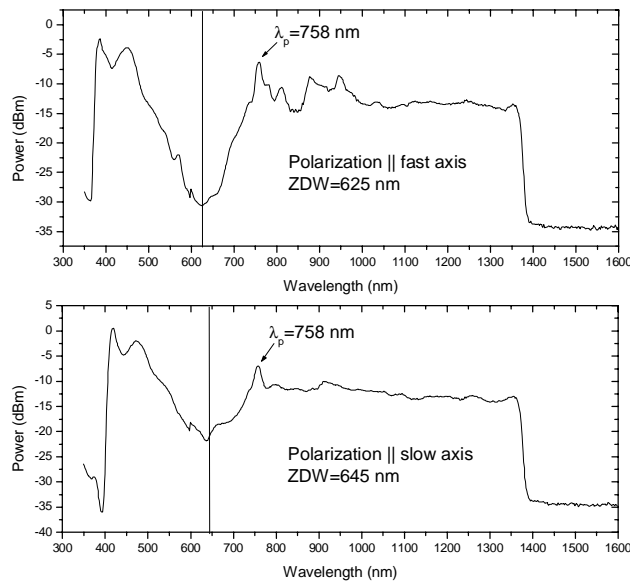
Fig. 2. Generated supercontinua along the two eigenpolarization axes of the fiber shown in Fig. 1. The upper spectrum was generated along the fast axis while the lower spectrum was generated along the slow axis. The dip on those spectra indicates that the fast axis has a ZDW of 625 nm while the slow axis has a ZDW of 645 nm.

After setting the input polarization parallel to the slow axis (ZDW=645 nm), we recorded the evolution of the generated spectrum as the injected intensity in the fiber increases for two pump wavelengths (740 nm and 758 nm in Figs. 3 and 4 respectively). These graphs are composed of 63 spectra recorded after each incremental increase of the input intensity. The graph of the injected intensity dependence of the supercontinuum provides an unambiguous evidence that the fission of higher-order solitons is indeed responsible for the initial broadening of the spectrum. One can see that for low injected intensities, very little broadening is observed but a single fundamental soliton is rapidly emitted and strongly redshifted as the power increases. In Fig. 3, a second fundamental soliton is emitted at roughly 6 GW/cm^2 of injected intensity and as the latter is further increased, so does the number N of fundamental solitons propagating in the fiber and these solitons extend further in the infrared region. On the shorter wavelength side of the spectrum, the evolution of the phase-matched

non-solitonic radiation can also clearly be seen [12]. Note that the features present in the extreme left of the spectra in Figs 3 and 4 (around 400 nm) even at low injected intensities are only artifacts attributable to the second order of the diffraction grating and do not represent real frequencies generated in the fiber.

Besides the fact that the inspection of Figs. 3 and 4 confirms that the fission of higher-order solitons is indeed the mechanism responsible for the initial broadening of the supercontinuum, these results also clearly show that at a certain point as the input intensity is increased, other nonlinear effects such as four-wave mixing help to flatten the spectrum by filling the gaps left between the solitons and the NSR in the visible part of the spectrum. As of now, it is known that a broad supercontinuum is achievable at the expense of sacrificing the flatness. Previous work has shown that pumping with sufficient power in the anomalous regime, but relatively far from the ZDW, can lead to a very broad supercontinuum, but the latter always suffers from a large gap around the ZDW [13]. On the other hand, this gap can be narrowed by pumping close to the ZDW as the much smaller dispersion will enhance the FWM efficiency and thus generate more frequencies in the gap region [9]. Another way to fill the gap around the ZDW would be to shorten the fiber in order to increase the efficiency of the FWM process between the redshifted solitons and the blueshifted NSR [9]. Concerning the influence of the pump wavelength on the width of the generated supercontinuum, it is worth noting that in Fig. 4, where the pump wavelength is farther from the ZDW than it is in Fig. , the width is limited by the strong OH absorption peak at 1380 nm.
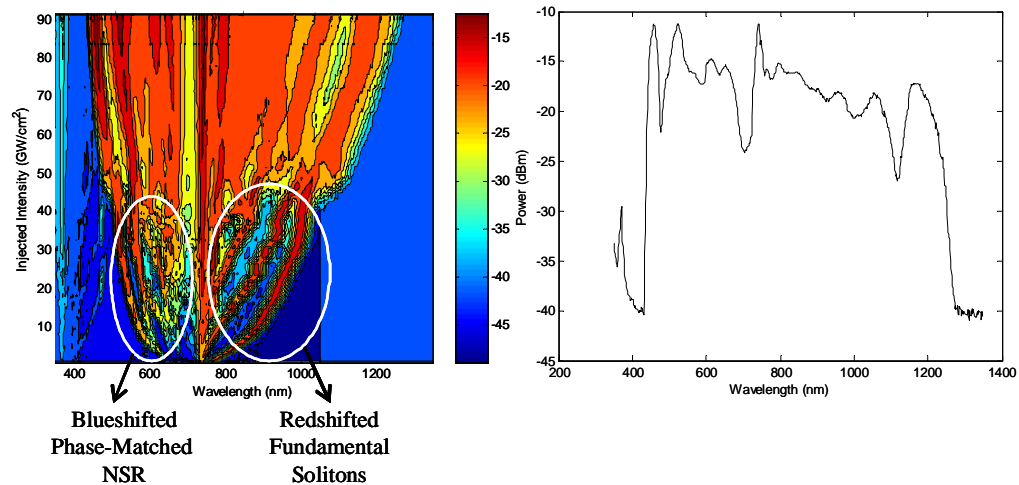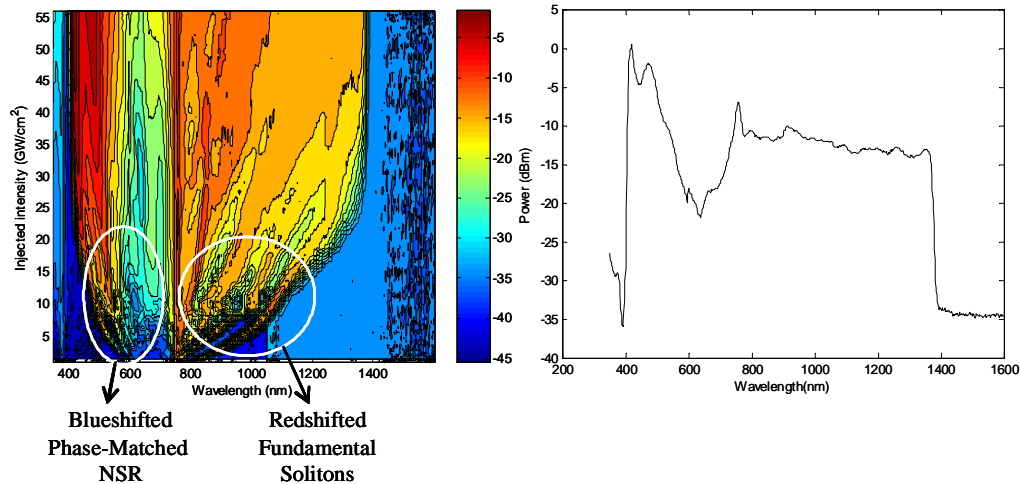

Fig. 3. (529 KB) Evolution of the generated spectrum as the injected intensity is increased. The pump wavelength was λ=740 nm, the pulse duration Δt_{FWHM}=127 fs and the polarization was oriented along the slow axis of the fiber. On the right is shown a detailed view of the supercontinuum generated at 91 GW/cm^2 of injected intensity (P_o=2.7 kW).

Fig. 4. (508 KB) Evolution of the generated spectrum as the injected intensity is increased. The pump wavelength was λ=758 nm, the pulse duration Δt_{FWHM}=192 fs and the polarization was oriented along the slow axis of the fiber. On the right is shown a detailed view of the supercontinuum generated at 56 GW/cm^2 of injected intensity (P_o=1.7 kW).

To investigate the influence of the input polarization on the generated supercontinuum, the input polarization was incrementally rotated and the changes in the spectrum were monitored. The input conditions were similar to those leading to the results shown in Fig. 4: we used a 2 m long section of the MS fiber shown in Fig. 1, the input laser had a pulse duration of 192 fs and a wavelength of 758 nm. Figures 5(a), 5(b) and 5(c) display the evolution of the generated spectra as a function of the input polarization orientation for injected intensities of 60 GW/cm^2, 20 GW/cm^2 and 10 GW/cm^2 respectively. A total of 100 spectra were recorded and used to compose each graph.

In Fig. 5(a), the injected intensity of 60 GW/cm^2 is sufficient to yield a broadband supercontinuum for both axes of the fiber, but as the intensity is decreased to 20 GW/cm^2, the fast axis having a smaller ZDW does not produce a supercontinuum anymore (Fig. 5(b)) and by further reducing the intensity to 10 GW/cm^2, neither axes can generate a flat and broadband supercontinuum (Fig. 5(c)). This behavior stems from the fact that the pump wavelength is located farther away from the ZDW along one polarization axis (~133 nm for the fast axis vs 113 nm for the slow axis) and the farther the pump wavelength is from the ZDW, the greater the required intensity is to generate a flat supercontinuum. In Fig. 5(b), the stronger dispersion along the fast axis at 758 nm limits the FWM efficiency required to flatten the spectrum while substantial broadening is observed along the slow axis. Also, a stronger dispersion at the pump wavelength implies a lower number N of fundamental solitons thus making it more difficult to fill the larger gaps left in the spectrum (see eq.1). As a result, only the initial broadening attributable to the fission of solitons can be observed along one polarization axis with the available injected intensity while the other axis can generate a supercontinuum.
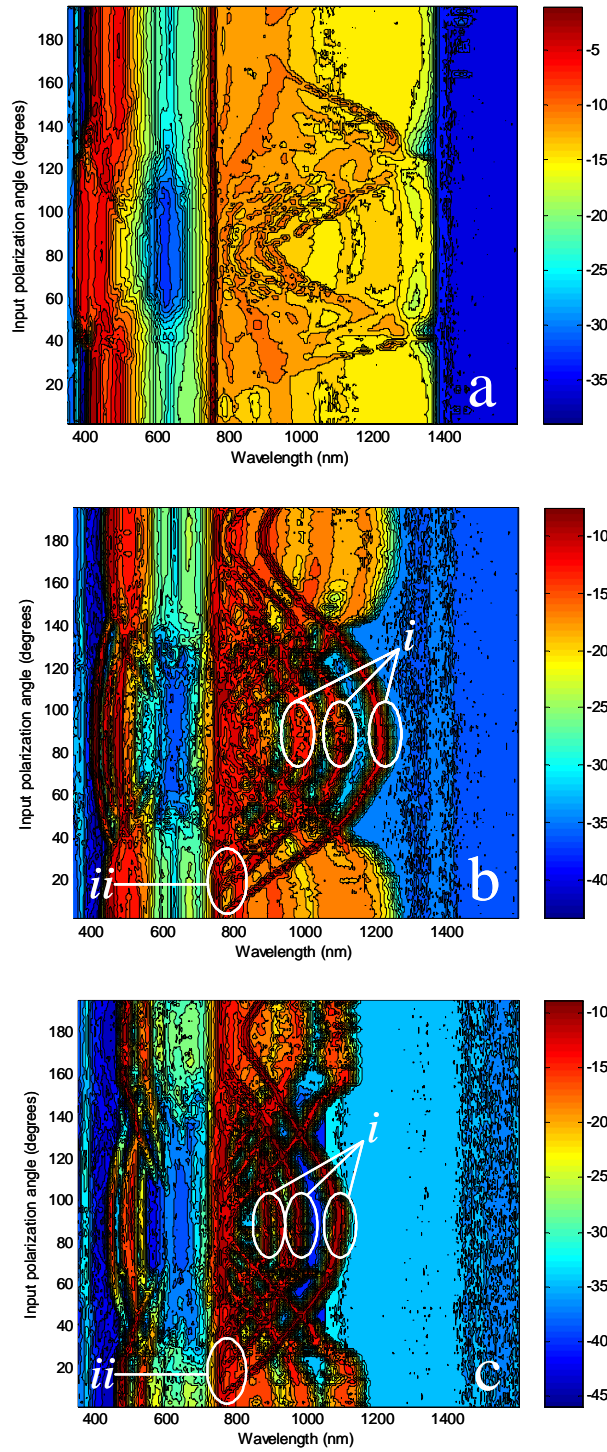
Fig. 5. Evolution of the generated spectrum as the input polarization is rotated. The 0^0 position was aligned with the slow axis of the fiber. The input pulses had a wavelength λ=758 nm, the pulse duration Δt_{FWHM}=192 fs and the injected intensity was 60, 20 and 10 GW/cm^2 for a, b and c respectively.

It has been reported elsewhere that for a birefringent MS fiber, the spectral components created along a polarization axis of the fiber maintain their polarization during the propagation [13]. The results presented in the current article strongly support this observation. Indeed, perhaps the most notable feature of the graphs shown in Fig. 5 is that the soliton behavior, while rotating the input polarization, demonstrates that the spectral components generated in either axis are not coupled to those in the other axis. This is attributable to the strong birefringence of the fiber which implies that after only a few millimeters of propagation, the pulses along the two polarization axes do not interact anymore. The resulting spectrum, at the output of the fiber, thus consists of the superposition of the supercontinua generated along each polarization axis. By inspection of Figs 5(b) and 5(c), one can clearly see that the redshifted components along the fast axis (i) return toward the pump wavelength at 758 nm as the input polarization is rotated. After a 90^0 rotation, so that the polarization is now oriented along the slow axis of the fiber core, the strongly redshifted solitons that were present on point (i) disappeared totally and came back to the pump wavelength (ii), implying that no spectral broadening occurs anymore along the fast axis around the 0^0 position on the graph. Meanwhile, the opposite process occurred along the slow axis as new solitons emerged from the pump while the polarization was rotated from the 90^0 position on the graph and they evolved to form a supercontinuum along the slow axis at the 0^0 position. Thus, if the input polarization is not exactly aligned along one of the polarization axes of the fiber, all of the energy coupled to the other eigenpolarization mode of the fiber can be considered as energy that cannot contribute to efficiently generate a supercontinuum along that axis and this energy will cause a more or less important broadening along the other axis depending on how much energy is coupled into it.

3. Conclusion

We have presented experimental results on SCG in a highly birefringent and highly nonlinear MS fiber. Our results confirm that the initial broadening in the supercontinuum generation process is indeed due to the fission of higher-order solitons into redshifted fundamental solitons along with blueshifted non-solitonic radiation. By monitoring the generated spectrum while incrementally increasing the injected power in the fiber, we were able to establish a detailed scenario of the evolution of the supercontinuum. By similarly collecting the spectrum while rotating the input polarization, we have clearly demonstrated that the resulting supercontinuum is made of the superposition of the generated frequencies in each distinct eigenpolarization mode of the fiber. The format in which the experimental results were presented provide a valuable insight on the mechanism underlying the initial broadening in the SCG process for highly birefringent MS optical fibers, although there is still room for further work in order to get a better understanding of the dynamics that governs the subsequent flattening of the spectrum. Further enlightment, both theoretical and experimental, on this aspect is indeed called for, in view of some potential applications of SCG such as optical coherence tomography, optical metrology and sensor technology.